# PROBABILISTIC PERFORMANCE ASSESSMENT: SCC OF SNF INTERIM STORAGE CANISTERS

C. Bryan[1], C. Sallaberry[1], R. Dingreville[1], C. Stockman[1], H. Adkins[2], and M. Sutton[3]

[1]Sandia National Laboratories, P.O. Box 5800 Albuquerque, NM 87185.  crbryan@sandia.gov
[2]Pacific Northwest National Laboratory, P.O. Box 999, Richland, WA 99352
[3]Lawrence Livermore National Laboratory, 7000 East Ave., Livermore, CA 94550

*For long-term storage, spent nuclear fuel (SNF) is placed in dry storage cask systems, commonly consisting of welded stainless steel containers enclosed in ventilated cement or steel overpacks. At near-marine sites, failure by chloride-induced stress corrosion cracking (SCC) due to deliquescence of deposited salt aerosols is a major concern. This paper presents a preliminary probabilistic performance assessment model to assess canister penetration by SCC. The model first determines whether conditions for salt deliquescence are present at any given location on the canister surface, using an abstracted waste package thermal model and site-specific weather data (ambient temperature and absolute humidity). As the canister cools and aqueous conditions become possible, corrosion is assumed to initiate and is modeled as pitting (initiation and growth). With increasing penetration, pits convert to SCC and a crack growth model is implemented. The SCC growth model includes rate dependencies on temperature and crack tip stress intensity factor. The amount of penetration represents the summed effect of corrosion during time steps when aqueous conditions are predicted to occur. Model results and sensitivity analyses provide information on the impact of model assumptions and parameter values on predicted storage canister performance, and provide guidance for further research to reduce uncertainties.*

## I. INTRODUCTION

Following initial cooling in pools, spent nuclear fuel (SNF) is transferred to dry storage casks for longer-term storage at the reactor sites. The storage cask systems are commonly welded stainless steel[1] containers enclosed in ventilated concrete or steel overpacks. These cask systems are intended as interim storage until a permanent disposal site is developed, and until recently, were licensed for up to 20 years, and renewals also up to 20 years. In 2011, 10 CFR 72.42(a) was modified to allow for initial license periods of up to 40 years, and also, license extensions of up to 40 years. However, the United States does not currently have a disposal pathway for SNF, and these containers may be required to perform their waste isolation function for many decades beyond their original design criteria. Of primary concern with respect to the long-term performance of the storage casks is the potential for canister failure due to localized corrosion. For most dry cask storage systems, passive ventilation is utilized to cool the casks within the overpacks, and large volumes of outside air are drawn through the system. Dust and aerosols within the air are deposited on the steel canisters, and as the casks cool over time, salts in the dust will deliquesce to form brine on the storage container surface. Under these conditions, localized attack can occur. Chloride-induced stress corrosion cracking (SCC) of welded zones is of special concern, as it is a well-documented mode of attack for austenitic stainless steels (including 304SS and 316SS) in marine environments[2], and many independent spent fuel storage installations (ISFSIs) are located in coastal areas. Recent canister inspections[3,4] have shown that chloride salts are present on the surface of in-service canisters in near-marine settings. However, canister surface inspections of sufficient resolution to detect SCC have never been carried out, because access to the canister surfaces through vents in the overpacks is extremely limited, and high radiation fields make removal of the canisters from the overpacks undesirable. Here, the available information on the canister surface environment and experimental and observational experience with stress corrosion cracking of stainless steels is utilized to develop a probabilistically-based model for evaluating the potential for SNF interim storage canister failure by through-wall SCC.

## II. CRITERIA FOR SCC

In order for SCC to occur, three criteria must be met: the metal must be susceptible to SCC, an aggressive environment must exist, and sufficient tensile stress must be present to support SCC. In general, these criteria are expected to be met, at least at some ISFSI sites, during the period of interim storage, especially if the development of a repository for final disposal is delayed. Although SCC of interim storage canisters has never been observed, that may be largely canister surface inspections capable of

detecting SCC have never been performed. The welded interim storage canisters are made of austenitic stainless steels which are susceptible to SCC, and susceptibility is higher in the heat affected zones (HAZ) of welds. Recent studies at three sites[3,4] have shown that chloride salts are present on the canister surfaces; if temperatures drop sufficiently for salt deliquescence, a corrosive aqueous environment could potentially occur. Finally, tensile stresses will be present in the canisters due to welding and fabrication. Residual stresses in SNF interim storage canisters have never been measured; however, weld residual stress modeling conducted by the Nuclear Regulatory Commission (NRC)[5] indicates that through-wall tensile stresses of sufficient magnitude to support SCC are likely to exist in weld HAZ.

When data to support a deterministic performance assessment are sparse or inadequate, a probabilistic performance assessment model is often used. Probabilistic models allow more accurate depiction of parameter uncertainties, while also offering a powerful tool to importance of these input uncertainties. Here, a probabilistic model for SCC of interim storage canisters is developed and presented. To make the problem tractable with the resources available, many simplifying assumptions have been made, and the scope of the model has been restricted.

The SCC model presented here evaluates the environmental conditions on the storage canister surface as a function of location on the surface and time, and determines when the environmental conditions at a given location support localized corrosion. Then, corrosion is initiated, first as a pit because experimental and observational studies have shown that SCC initiate from corrosion pits, and then transitioning into a stress corrosion crack. Pit and crack growth rates are a function of the environment, and are calculated for each location at each time interval. As discussed elsewhere in this report, the performance failure criterion is the development of a through-wall crack. Predicted SCC depths were tracked at different locations on the canister surface until penetration is predicted to occur, or for the first 100 years of storage, whichever occurs first.

## III. ENVIRONMENT MODEL

The environment at any given location on the storage canister surface will be aggressive if two criteria are met: a corrosive chemical species is present, and aqueous conditions exist. For this model, the aggressive species is assumed to be chloride.

A third potential criterion for a corrosive environment may be the amount of chloride present. Several studies[6,7,8,9,10,11] have shown that there may be a lower limit on the amount of chloride on the package that can support SCC initiation—however, these limits are low, ranging from 0.3 to 0.005 g m$^{-2}$. The United Kingdom Nuclear Decommissioning Authority has issued cautious operational limits for chloride surface concentrations on 316L waste packages of 0.01 g/m$^2$ for temperatures between 10 and 30°C and 0.001 g/m$^2$ for temperatures between 30 and 50°C[12]. Given these low values, it is unlikely that low chloride surface load will effectively limit the initiation of SCC.

However, it is also possible that continued SCC growth after initiation is a function of the surface salt load, because it affects the current carrying capacity of the brine layer and the ability of the cathode, outside of the crack, to support corrosion at the anode, within the crack. This approach has been proposed for estimating maximum pitting penetration depths in several recent papers[13,14,15], but has never been applied to SCC.

### III.A. Presence of Chloride

The greatest concern of SCC is at near-marine sites, so the assumption is made in this model that *the deposited salts are chloride-rich sea-salts*. It is known that sea-salts will deposit on canisters at least at some near-marine ISFSIs; aggregates of sea-salts were observed in dusts collected from in-service storage canister surfaces at Diablo Canyon, on the California coast[4]. It is also assumed that the chloride is present immediately upon canister emplacement into storage, and that the rate of chloride loss due to degassing and particle-gas conversion reactions is less than the rate of deposition. Therefore, conditions for localized corrosion of the canister surface are assumed to occur any time that aqueous conditions are predicted on the canister surface. The deliquescence properties of the deposited salts are also assumed to be those of sea-salts.

### III.B. Aqueous Conditions Submodel

Localized corrosion cannot occur unless an aqueous film is present on the metal surface. Within the shelter of the overpack, a persistent aqueous solution can only form by deliquescence of salts on the canister surface. Deliquescence occurs when the activity (chemical potential) of water in the atmosphere is equal to the activity of water in a saturated solution of the salt (or the salt assemblage) on the canister surface. The activity of water in air is equal to the relative humidity (RH), expressed as a unit value, and the RH at which deliquescence occurs is the deliquescence RH (RH$_D$).

However, a bulk aqueous solution is not required for corrosion. An adsorbed water film is sufficient, and experimentally, corrosion is commonly observed at an RH significantly lower than the RH$_D$. The RH at which corrosion is observed is referred to as the limiting RH, or RH$_L$. At any given point on the canister surface, corrosion can occur, or progress, if the location- and timestep-specific RH is greater than the RH$_L$. The

derivation of RH and $RH_L$ is described in the sections below.

Because SCC can only occur where there is sufficient tensile stress, and that condition is only likely to occur near welds, a weld-location model has also been developed, and identifies the locations at which aqueous conditions must be evaluated.

### III.B.1. Submodel for Location-Specific RH on the Canister Surface

The location-specific RH values can be calculated from two parameters: the canister surface temperature at any given location; and the absolute humidity (AH), or water content, of the inflowing air.

*Canister surface temperature submodel.* To determine location-specific canister surface temperatures through time, maps of canister surface temperatures were calculated using a specific set of values for storage system design (horizontal); the fuel loading (number and geometry of assemblies); the fuel burnup; the heat load (corresponding to a given time out of reactor), and a single fixed ambient external temperature. The parameter values used are described elsewhere[16]. Decay heat loads were varied to represent waste emplaced into dry storage at different times out of the reactor. However, a single curve for heat generation as a function of time-out-of reactor, corresponding to a single fuel burn-up, was used. Hence, variations in fuel burnup are not considered.

The thermal modeling provided temperature maps of the canister surface (for example, Figure 1) for each of 8 decay heat loads corresponding to different lengths of time out of the reactor, for a single ambient temperature of 15.6ºC (60ºF). To abstract this for the SCC model, canister surface temperatures for each decay heat load were extracted at 35 positions on the canister surface. By interpolating between those 35 grid points, the temperature at any point on the canister surface was estimated for a given decay heat load. To obtain the surface temperature at any location as a function of time, interpolation was done between temperature maps representing different heat loads (times out of the reactor).

The SCC model time-step was one day. Daily mean ambient temperatures for the simulation period of 100 years were calculated by sampling from a distribution fitted to one year of measured data from a relevant NOAA weather station. Then, the difference between the predicted ambient temperature and the nominal ambient temperature used in the thermal modeling (15.6ºC) was applied as a delta to the surface temperatures provided by the canister thermal model. This yielded the temperature used in that time step of the SCC model, for the location of interest on the canister surface.
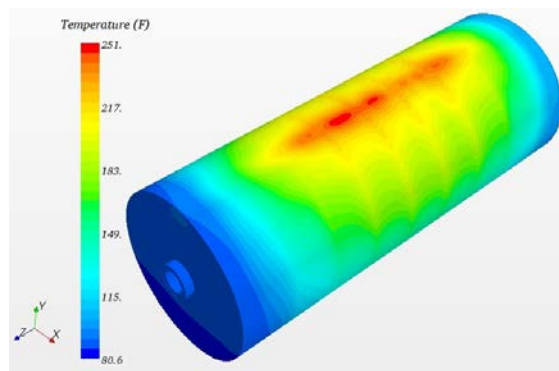


Fig. 1. Canister surface temperature map, for a decay heat load of ~7.6 kW[16].

*Absolute humidity submodel.* Similarly to the ambient temperature, the predicted AH is based on one year of NOAA data from the same weather station. Based on the measured NOAA data, the predicted offsets for the ambient temperature and the AH are correlated with a coefficient of correlation of 0.6.

Given the location-specific temperature and the AH of the incoming air, the RH at any point on the surface of the canister can be calculated.

### III.B.2. $RH_L$ Parameter

The $RH_L$ is the relative humidity at which corrosion can occur. It is a function of the salt assemblage on the canister surface, and is generally somewhat below the deliquescence RH for the salt assemblage. Sea-salts are generally considered to deliquesce at ~30% RH, but corrosion has been observed on metal coupons covered with sea-salts at RH values as low as 15% (Ref 17). Because it is assumed that chloride is present as sea-salts for this model, the $RH_L$ is assumed to be 15%. However, it should be noted that there is some evidence of a temperature dependence for $RH_L$, that is not captured here.

Given AH and the waste package surface temperature, the location-specific RH is calculated by converting the AH to the water vapor pressure and dividing by the saturated vapor pressure at the temperature of interest. At high initial temperatures, only very low surface RH values are possible. As the decay heat load drops and the storage canister cools, the temperature drops and for any given AH, the RH increases. The maximum value of AH from the NOAA site data used in this model is about 25 $g/m^2$. This corresponds to an RH of 15%, equivalent to the $RH_L$, at about 60ºC, indicating that this is the approximate maximum temperature at which conditions for corrosion exist, for the ambient weather data used in this model.

*III.B.1. Submodel for Weld Locations*

The surface temperature maps and ambient AH values allow one to evaluate the RH and potential occurrence of corrosion at any point on the canister surface. However, the only points where SCC is likely to occur are in weld HAZ. For this model, it is assumed that the canisters were made in two sections, with two longitudinal welds randomly located with respect to each other, and a circumferential weld bisecting the canister in the exact center. There are also base plate and lid welds at each end. For this version of the SCC model, only the longitudinal welds are considered; the circumferential weld and the baseplate and lid welds are not evaluated.

When canisters are placed in overpacks, the locations of the welds relative to the overpack are not recorded. Here, the locations of the two longitudinal welds are treated as aleatory uncertainty, and are sampled, independently, each realization. The welds are discretized into 10 cm sections, and at each time step, temperature and RH are calculated for the center of each section. If the RH is larger than $RH_L$, conditions for corrosion are assumed to exist.

### III.C. Susceptible Material Submodel

SNF dry storage casks currently in use are made from austenitic stainless steels, including 304, 304L, 316, and 316L, with the predominant material being 304. Should sufficient tensile stress occur (Section III.D), these stainless steels are susceptible to SCC in aggressive environments. It occurs readily in experimental tests with deliquesced sea-salts[18,19,20,21], and has also been observed in near-marine ambient temperature field tests and industrial sites[2,22,23,24]. However, the degree of susceptibility is a function of several factors, including the degree of sensitization, the degree of cold work, the presence of iron contamination on the metal surface, and the surface finish[25].

- Sensitization—the degree of sensitization has not been measured in representative storage canister welds, but it is likely that sensitization occurs, because of the metal thickness (5/8") and the need for multiple weld passes to make the weld. For the SCC model developed here, it is assumed that the effects of sensitization are included implicitly, because the corrosion rate data used to parameterize the SCC model include data from weld and HAZ samples and from samples that were deliberately sensitized.
- Cold working—As with the effects of sensitization, we assume that the effects of cold working are implicitly included in the SCC model presented here, through the corrosion rate data.
- Iron contamination—For this study, the potential effects of iron contamination are ignored.

- Surface finish—A rough surface finish (>1 µm) can promote initiation of corrosion, apparently by trapping water and chloride ions on the surface (Parrott and Pitts 2011). Here, the potential effects of variable surface finishes are ignored.

### III.D. Tensile Stress Submodel

In order for a SCC to grow, tensile stress is required. For the model presented here, it is assumed that only residual stresses related to welding are sufficient to promote SCC. There are no direct measurements of residual stresses associated with typical SNF dry storage casks welds, although Sandia National Laboratories is planning to assess the residual stresses in a full-diameter cylindrical canister mockup in 2015. The through-wall stress profiles used here are from weld residual stress modeling performed by the NRC[5]. The stress profiles were calculated for longitudinal canister welds, and are those for tensile stresses parallel to each weld, which are largest and which are tensile, and in fact, greater than the uniaxial yield stress, throughout the wall thickness. The NRC[5] evaluated both isotropic and kinematic hardening laws, and noted that the real stresses would lie between the two model profiles. For the probabilistic model described here, the kinematic and isotropic model curves for the longitudinal welds were discretized, and a stress curve was generated by linearly interpolating a randomly generated position between the curves for the two models. For each realization, a value *x* between 0 and 1 was sampled, the isotropic curve was multiplied by *x* and the kinematic curve by (1-*x*), and the results are added together. The summed curve was used in that realization.

### IV. STRESS CORROSION CRACKING MODEL

The SCC model presented here tracks the conditions at weld locations on the canister surface, and initiates corrosion once the $RH_L$ has been exceeded and nominally aqueous conditions are predicted to exist. After initiation of corrosion, further penetration occurs only during time-steps when the $RH_L$ is exceeded. The stress corrosion cracking model used here is based on that of Turnbull et al.[26,27], and the major features of the model are described in those publications. The Turnbull model assumes that SCC originate at corrosion pits, a commonly accepted view that has a great deal of experimental support[6,7,18,21,22,26,28]. The model has several submodels:

- Pitting initiation model
- Pitting growth model
- Model for pit-crack transition
- Model for crack growth

Each of these models will be discussed below.

## IV.A Pit Initiation Model

The sub-model used for pitting initiation is based on nucleation-type theory in conjunction with the statistical methods used to describe rare-event processes when conditions for SCC are met[26]. However, very few observed data are reported in the literature in terms of the environment of interest for this study and what is usually reported is the maximum pit depth observed rather than the evolution of pit depth as a function of time, rendering the model by Turnbull et al.[26] difficult to parameterize for the present study. Rather, we have implemented a statistical approach for the formation of stable pits, considering both pit growth and pit death. However, because of the paucity of data for relevant environmental conditions, the current model has been parameterized to result in instant stable pit formation, reducing greatly any incubation time. While conservative, this is consistent with experimental observations of rapid pitting and SCC in austenitic stainless steels when exposed to deliquesced salts.

## IV.B Pit Growth Model

The pitting growth model that is used is that described in Turnbull et al.[26]. It has the form:

$$x_{pit} = \alpha_{pit} t^{\beta_{pit}} \tag{1}$$

Where $x_{pit}$ is stable pit depth, $t$ is time after initiation, $\alpha_{pit}$ is a scaling factor, and the exponent $\beta_{pit}$ is, in part, a function of the pit geometry and determines the shape of the growth curve with time. Parameters $\alpha_{pit}$ and $\beta_{pit}$ are generally determined experimentally for a given system. However, given the lack of relevant experimental data, a different approach was used. Some theoretical constraints can be placed on $\beta_{pit}$, which is a function of the pit geometry. For a fixed corrosion rate and a hemispherical pit, $\beta_{pit}$ is equal to $^1/_3$. As pits deepen, the corrosion rate changes and becomes controlled by diffusion into and out of the pit. At this point, $\beta_{pit}$ is equal to ½. Literature data define the likely range of $\beta_{pit}$ from 0.3 to 0.5 (Ref. 29). For this model, $\beta_{pit}$ is uniformly sampled over that range. Then $\alpha_{pit}$ is determined. This parameter is strongly controlled by the environment of corrosion, and relevant data are not available. Instead, we make use of the experimental observation that pits transition to stress corrosion cracks at depths of 50-70 µm. This transition occurs, according to the pit-to-crack transition model implemented here, when the pit growth rate, which decreases with depth, is equal to the calculated crack growth rate, which increases with depth[28]. Therefore, for each realization, the pit growth parameter $\beta_{pit}$ is randomly selected from 0.3–0.5, and the pit growth parameter $\alpha_{pit}$ is chosen such that the pit growth rate is equal to the calculated crack growth rate (Section IV.D) for that realization and time step, at a randomly selected depth of 50-70 um.

## IV.C Pit-to-Crack Transition Model

As a corrosion pit grows, it acts as a stress focuser, and should SCCs form, they are commonly observed to originate from corrosion pits[6,7,18,21,22,26,28]. The depth at which the transition from pit to crack occurs is generally based on one of two criteria[29]:

- the calculated stress corrosion crack growth rate (as described in the following section), which increases with depth because it is a function of the crack tip stress intensity factor ($K$), exceeds the corrosion pit growth rate, which decreases with depth[28];
- the pit depth increases to the point that the equivalent surface crack would have a $K$ value that exceeds the threshold stress intensity factor ($K_{th}$) for SCC growth.

The model implemented here is that described in Turnbull et al.[26] uses the Kondo[28] criterion. To do this, both growth rates are calculated each time step, and the pit is assumed to transition to the crack when the crack rate exceeds the pit rate. It should be noted that this model is a simplification; recent studies have shown that cracks sometimes initiate on pit sides rather than pit bottoms, due to localized stress concentrations[29,30,31].

## IV.D Crack Growth Model

SCC crack growth rates are a function of many different factors and can be expressed in the following general form (for example, EPRI 2011; Wu and Modarres, 2012; EPRI, 2014):

$$\frac{dx_{crack}}{dt} = \dot{x}_{crack} = \tag{2}$$

$$\alpha_{crack} \cdot f(T) \cdot f(K) \cdot f(R_a) \cdot f([Cl^-]) \cdot f(pH) \cdot f(\sigma_{ys}) \dots$$

Where $\alpha_{crack}$ is the crack growth amplitude factor (or, the crack growth rate at a fixed reference set of conditions), and that value can be modified by many other factors, including material property factors such as the stress intensity factor ($K$), degree of sensitization ($R_a$), and yield stress ($\sigma_{ys}$); and environmental factors such as temperature ($T$), chloride concentration ($[Cl^-]$), the mass of chloride per unit surface area ($m_{Cl}$), and the solution pH.

The effects of $K$ and T are included in the model presented here; the other factors are not considered explicitly, but are included implicitly in the experimental data sets used to parameterize the SCC growth rate. The

experimental data sets include base metal, weld, HAZ, and sensitized samples, and both 304 and 304L, capturing the effects of different $R_a$ and $\sigma_{ys}$ values. Similarly, the experimental data are based on samples exposed to sea-salts and sea-spray at different RH conditions, matching the conditions of interest; therefore [Cl⁻] and solution pH are implicitly included in the model.

For a model accounting for $K$ and $T$, a power law dependence is assumed for K, while an Arrhenius relationship is assumed for the temperature dependence[32]:

$$\frac{dx_{crack}}{dt} = \tag{3}$$

$$\alpha_{crack} \cdot exp\left[-\frac{Q}{R}\left(\frac{1}{T}-\frac{1}{T_{ref}}\right)\right] \cdot (K-K_{th})^{\beta_{crack}}$$

where:

$dx_{crack}/dt$ is the crack growth rate
$\alpha_{crack}$ is the crack growth amplitude
$Q$ is the activation energy for g=crack growth
$R$ is the universal gas constant (8.314 J mol⁻¹ K⁻¹)
$T$ is the temperature (K) of interest
$T_{ref}$ is a reference temperature (K) at which $\alpha$ was derived. To be consistent with the PNNL thermal model, a reference temperature of 15.55ºC (60ºF) is used as the reference temperature.
$K$ is the crack tip stress intensity factor
$K_{th}$ is the threshold stress for SCC
$\beta_{crack}$ is the stress intensity factor exponent.

The above equation is implemented in this report. For a cracked structure under remote or local loads, the stress intensity factor ($K$) is a measure of the stress field ahead of the crack. In elastic fracture mechanics, when the applied value of the stress intensity factor exceeds the material's critical value, crack advance occurs. For subcritical cracking, the process of crack advance is linked to the applied value of the stress intensity factor through curve fits that are based on extensive experimental data. The stress intensity factor $K$ is defined as[32]:

$$K = \sigma_{applied}Y\sqrt{\pi x_{crack}} \tag{4}$$

Where $\sigma_{applied}$ is the tensile stress from the weld residual stress profile and $Y$ is a shape parameter, equal to 1 for an infinite flat plate. Given that the waste canister circumference and length are much, much greater than the thickness of the canister wall and the crack depth/length at the time of penetration, this is a reasonable approximation.

The threshold stress intensity factor for SCC, $K_{th}$, was estimated to be 1.97 MPa m^½, the minimum value of K for a crack of depth 25 µm, the minimum stable pit size. Uncertainty in $K_{th}$ has little impact on model results, as the estimated tensile stresses (Section III.D) are very large.

The stress corrosion cracking growth rate model is parameterized by fitting experimental rates determined for atmospheric SCC under ambient and high temperature conditions for 304 and 304L stainless steels (Figure 2). A detailed description of the parameterization of the SCC crack growth model is beyond the scope of this paper; however the basic approach was to sample $\beta_{crack}$ over the range 0–1 (based on literature values), and then to invert equation 3, sampling crack growth rates and activation energies, with uncertainty, over the range defined by experimental data (Figure 2), to estimate $\alpha_{crack}$.
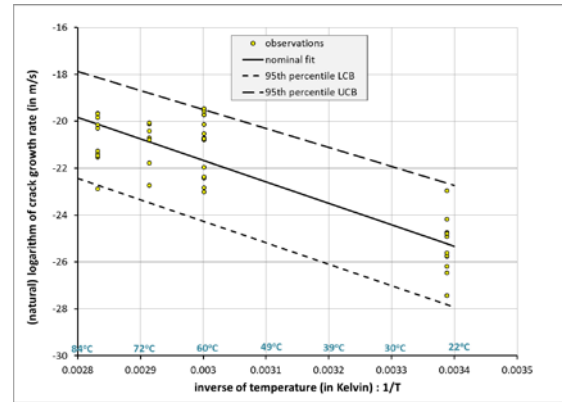


Fig. 2. Experimental data used to parameterize the SCC crack growth model[6,22,23,24,33], and confidence interval based on that data.

## V. RESULTS

Predicted penetration times for the SCC model described here are not provided; the intent of this version of the model was to build the general form and to assess the impact of individual parameters. Because of the limited data to support model parameterization, the predicted penetration times are probably not accurate. Also, very conservative assumptions were made for two of the three criteria for SCC, corrosive environment and sufficient tensile stress. The assumption of the presence of sea-salts, and of no *de minimus* value for SCC initiation or propagation, greatly reduces the possible use of environmental conditions as a screening criterion for SCC. The use of the highly tensile NRC[5] weld residual stress profiles is forced due to lack of alternative data, but is also highly conservative. Also, it should be noted that insufficient data were available to develop a good model

for SCC incubation time (e.g., pit initiation and growth, and conversion to SCC); the incubation time was conservatively assumed to be very short. Finally, only an example set of weather data was used, and applying this model to any real ISFSI site would require using site-specific weather data.

Despite this, the model results do provide some insights into the importance of parameter uncertainties.

- Predicted penetration rates are strongly sensitive to parameters describing the SCC crack growth rate. As seem in Figure 2, the uncertainty in the possible range of rates covers several orders of magnitude, which also affects the activation energy for SCC, proportional to the slope of the data in Figure 2. The crack growth data used here are for cracks in small samples, and in many cases, correspond to early crack growth rates. Some recent studies suggest that crack growth rates slow with increasing crack depth, possibly due to increasing limitations in transport between the anode in the crack and the cathode on the surface as the crack deepens[6,19]. However, this conclusion is inconsistent with widely-used models for crack growth such as Equation 3, which predict increasing crack growth rates with crack depth. Moreover, experimental artifacts may have contributed to the slower crack growth rates observed at greater crack depths in those studies.
- The choice of $RH_L$ at which corrosion occurs dramatically affects predicted corrosion times. This is generally taken to be 15% but is not well constrained as a function of temperature. Using a value of 20% doubled the predicted penetration times.
- High canister heat loads provide protection for only a few years. Effective passive ventilation produces large variations in canister surface temperature—the first area to experience cool enough temperatures to have deliquescence is where the first through-wall crack is predicted to occur.

## VI. CONCLUSIONS

The results of a pilot study to develop a probabilistic model for SCC of SNF interim storage canisters are presented. Although simplified, the basic approach has been developed and applied to an example case. The study illustrates the need for additional experimental efforts to allow quantitative evaluation of important processes (e.g., pit initiation and growth under atmospheric conditions), and to reduce uncertainties in important parameters such as SCC growth rate, limiting RH for corrosion, and weld residual stress profiles. Additional model development and parameterization is

required prior to applying it to SNF canisters at actual ISFI sites.

## REFERENCES

1. B. HANSON, H. ALSAED, C. STOCKMAN, D. ENOS, R. MEYER, and K. SORENSON, *Gap Analysis to Support Extended Storage of Used Nuclear Fuel*, FCRD-USED-2011-000136 Rev 0, U.S. DOE (2012).
2. R.M. KAIN, "Marine Atmospheric Stress Corrosion Cracking of Austenitic Stainless Steels"*, Materials Performance* **29**(12), 60 (1990).
3. ELECTRIC POWER RESEARCH INSTITUTE, *Calvert Cliffs Stainless Steel Dry Storage Canister Inspection.* EPRI, Palo Alto, CA (2014).
4. C. BRYAN and D. ENOS, *Analysis of Dust Samples Collected from Spent Nuclear Fuel Interim Storage Containers at Hope Creek, Delaware, and Diablo Canyon, California*, SAND2014-16383, Sandia National Laboratories, Albuquerque, NM (2014).
5. NUCLEAR REGULATORY COMMISSION (NRC), *Finite Element Analysis of Weld Residual Stresses in Austenitic Stainless Steel Dry Cask Storage System Canisters*, NRC Technical Letter Report (ADAMS ML13330A512) (2013).
6. K. SHIRAI, J. TANI, T. ARAI, M. WATARU, H. TAKEDA, and T. SAEGUSA, "SCC evaluation test of a multi-purpose canister." *in Proceedings 13th International High-Level Radioactive Waste Management Conference (IHLRWMC)*, Albuquerque, NM, American Nuclear Society, 824-831 (2011).
7. O. ALBORES-SILVA, E. CHARLES, and C. PADOVANI, "Effect of chloride deposition on stress corrosion cracking of 316L stainless steel used for intermediate level radioactive waste containers," *Corrosion Engineering, Science and Technology*, **46** (2), 124-128 (2011).
8. NRC, *Assessment of Stress Corrosion Cracking Susceptibility for Austenitic Stainless Steels Exposed to Atmospheric Chloride and Non-Chloride Salts.* NUREG/CR-7170. U.S. NRC (2014).
9. M. TOKIWAI, H. KIMURA, and H. KUSANAGI, "The amount of chlorine contamination for prevention of stress corrosion cracking in sensitized type 304 stainless steel," *Corrosion Science*, 25(8), 837-844 (1985).

10. M.F. TAYLOR, "The Significance of Salt Contamination on Steel Surfaces, Its Measurement and Removal," *UK Corrosion and Eurocorr 94* : 31 October-3 November, Bournemouth International Centre, UK (1994).

11. N. FAIRWEATHER, N. PLATTS, and D.TICE, "Stress-Corrosion Crack Initiation Of Type 304 Stainless Steel In Atmospheric Environments Containing Chloride: Influence Of Surface Condition Relative Humidity Temperature And Thermal Sensitization" *CORROSION 2008* (2008).

12. NUCLEAR DECOMMISSIONING AUTHORITY (NDA), *Industry Guidance - Interim Storage of Higher Activity Waste Packages – Integrated Approach.* NDA. West Cumbria, UK (2012).

13. Z. CHEN and R. KELLY, "Computational modeling of bounding conditions for pit size on stainless steel in atmospheric environments," *Journal of the Electrochemical Society*, **157**(2), C69-C78 (2010).

14. M.T. WOLDEMEDHIN and R.G. KELLY, "Evaluation of the maximum pit size model on stainless steel under atmospheric conditions," *ECS Transactions*, **58**(29), 41-50 (2014).

15. D. KROUSE, N. LAYCOCK, and C.PADOVANI, "Modelling pitting corrosion of stainless steel in atmospheric exposures to chloride containing environments," *Corrosion Engineering, Science and Technology*, **49**(6), 521-528 (2014).

16. PACIFIC NORTHWEST NATIONAL LABORATORY (PNNL), *Thermal Modeling of NUHOMS HSM-15 and HSM-1 Storage Modules at Calvert Cliffs Nuclear Power Station ISFSI*, PNNL-21788, Richland WA (2012).

17. M. MAYUZUMI, J. TANI, and T. ARAI, "Chloride induced stress corrosion cracking of candidate canister materials for dry storage of spent fuel" *Nuclear Engineering and Design*, **238**(5), 1227-1232 (2008).

18. G. NAYAKAMA, "Atmospheric stress corrosion cracking (ASCC) susceptibility of stainless alloys for metallic containers," *in Scientific Basis for Nuclear Waste Management XXIX*, **932**, 845-852 (2006).

19. J.I. TANI, M. MAYUZUMI, and N. HARA, "Initiation and propagation of stress corrosion cracking of stainless steel canister for concrete cask storage of spent nuclear fuel," *Corrosion* **65**(3), 187-194 (2009).

20. T.S. MINTZ, L. CASERES, X. HE, J. DANTE, G. OBERSON, D.S. DUNN, and T. AHN, "Atmospheric Salt Fog Testing to Evaluate Chloride-Induced Stress Corrosion Cracking of Type 304 Stainless Steel," *CORROSION 2012*: Salt Lake City, March 11-15, NACE (2012).

21. T. PROSEK, A. IVERSEN, and C. TAXEN, "Low temperature stress corrosion cracking of stainless steels in the atmosphere in presence of chloride deposits," *Corrosion*, **65**(2), 105-117 (2009).

22. A. KOSAKI, "Evaluation method of corrosion lifetime of conventional stainless steel canister under oceanic air environment," *Nuclear Engineering and Design*, **238**(5), 1233-1240 (2008).

23. H. HAYASHIBARA, M. MAYUZUMI, and Y. MIZUTANI, "Effects of temperature and humidity on atmospheric stress corrosion cracking of 304 stainless steel," *CORROSION 2008* (2008).

24. G. NAKAYAMA, and Y. SAKAKIBARA, "Prediction Model for Atmospheric Stress Corrosion Cracking of Stainless Steel," *ECS Transactions*, **50**(31), 303-311 (2013).

25. R. PARROTT and H. PITTS, *Chloride stress corrosion cracking in austenitic stainless steel: Assessing susceptibility and structural integrity*: U.K. Health and Safety Executive, RR902 (2011).

26. A. TURNBULL, L. MCCARTNEY, and S. ZHOU, "A model to predict the evolution of pitting corrosion and the pit-to-crack transition incorporating statistically distributed input parameters," *Corrosion Science*, **48**(8), 2084-2105 (2006).

27. A. TURNBULL, L. MCCARTNEY, and S. ZHOU, "Modelling of the evolution of stress corrosion cracks from corrosion pits," *Scripta materialia*, **54**(4), 575-578 (2006).

28. Y. KONDO, "Prediction of fatigue crack initiation life based on pit growth," *Corrosion*, **45**(1), 7-11 (1989).

29. X.-Y. ZHANG, S.-X. LI, and R. LIANG, "Effect of corrosion pits on fatigue life and crack initiation," *Proceedings ICF13* (2013).

30. A. TURNBULL, D. HORNER, and B. CONNOLLY, "Challenges in modelling the evolution of stress corrosion cracks from pits," *Engineering Fracture Mechanics*, **76**(5), 633-640 (2009).

31. A. TURNBULL, "Corrosion pitting and environmentally assisted small crack growth," *Proceedings of the Royal Society A: Mathematical, Physical and Engineering Science*, **470**(2169), p. 20140254 (2014).

32. G. WU, and M. MODARRES, "A Probabilistic-Mechanistic Approach to Modeling Stress Corrosion Cracking in Alloy 600 Components with Applications", *PSAM 2011* (2012).

33. A. COOK, N. STEVENS, J. DUFF, A. MISHELIA, T.S. LEUNG, S. LYON, J. MARROW, W. GRANTHER, and I. COLE, "Atmospheric-induced stress corrosion cracking of austenitic stainless steels under limited chloride supply," *Proc. 18th Int. Corros. Cong.*, Perth, Australia (2011).